

Experimental research of the effect of face milling strategy on the flatness deviations

Michał Dobrzynski¹, Daniel Chuchala¹✉ (orcid.org/0000-0001-6368-6810),
Kazimierz A. Orłowski¹ (orcid.org/0000-0003-1998-521X),
Mateusz Kaczmarczyk²

¹*Department of Manufacturing and Production Engineering, Faculty of Mechanical Engineering, Gdansk University of Technology, Gdansk, Poland*

michal.dobrzynski@pg.edu.pl, ✉ daniel.chuchala@pg.edu.pl,
kazimierz.orlowski@pg.edu.pl

²*Department of Innovativeness and Entrepreneurship, Faculty of Management, Warsaw University of Technology, Warsaw, Poland*

mateusz.kaczmarczyk77@gmail.com

Corresponding author: Daniel Chuchala

Email: daniel.chuchala@pg.edu.pl,

Address: Gdansk University of Technology, Faculty of Mechanical Engineering,
11/12 Gabriela Narutowicza Street, 80-233 Gdansk, Poland

Experimental research of the effect of face milling strategy on the flatness deviations

In this paper the dependencies between face milling strategy of EN AW6082-T6 aluminium alloy samples, with difference thicknesses (6, 8 and 12 mm) and two cold rolling directions, and flatness deviations were presented. Three strategies of milling included different proportions of material removed from both sides of the plates. This approach allowed to control the proportions of residual surface stresses on both sides of the specimens, which were created by the cold rolling process. The face milling strategy involving the symmetrical removal of material from both sides of the sample resulted in the best results of flatness deviations. This strategy was most effective for both rolling directions. It has been observed that the use of an appropriate face milling strategy is particularly important for thin sheets (6 mm thick). In the case of thicker plates (12 mm thick), the selected strategy has less impact on the final values of flatness deviations.

Keywords: milling, flatness, strategy, aluminium, surface, rolling, direction, residual, stresses,

Introduction

The light alloys, such as aluminium alloy, are willingly used in manufacture processes elements for automotive,^[1-3] aerospace^[4-5] and rail,^[6] because they are characterized by low density with sufficient strength.^[3] These properties allow saving fuel or electric energy during exploitation vehicles. The aluminium alloys are also often used to manufacture front panels for electronic and/or electrical equipment which often are mounted in server cupboards.^[7] The material used to make the blanks for the front panels is usually aluminium alloy sheet, the nominal thickness of which is the same as the nominal final dimension or is very close to the final dimension (1 mm larger).

Where the nominal dimension of the plate thickness is the same as the nominal dimension of the final panel thickness, the required front surface machined is based on the allowance for plate thickness resulting from cold rolling process tolerances.^[8] Most

often, however, the plate thickness is slightly higher than the final panel thickness.

Another production solution, which reduces manufacturing costs, is to make such a panel in a single fixing. This involves processing the panel only on the front side and the back side remains with the raw surface. Unfortunately, such a solution carries the risk of a significant impact of residual stresses remaining after the cold rolling process on the panel's flatness, as well as errors in the spacing of holes and pockets, which will be caused by movements associated with panel deflection.^[7] The cold rolling process is crucial for manufacturing process of aluminium alloy sheet which gives specific properties to the processed material.^[9-10] This processing introduces anisotropic properties in the processed material. The anisotropy of the rolled material significantly affects the mechanical properties, as shown in the works.^[11-12] The cold rolling process deforms the material plastically. Although the cold rolling process is often followed by stress relieving processes, there are still residual stresses at the sheet surface.^[13-16]

Residual stresses occur on both sides of the sheet, which creates a certain balance to ensure the right shape and dimensions. Hattori et al.^[17] have shown that residual stresses after the cold rolling process of the aluminium alloy occur up to a depth of about 1 mm and reach up to 50 MPa. When machining the surface of thin sheets (up to 12 mm thick), the removal of a layer with residual stresses on one side of the sheet may lead to deformation of the component due to the residual stresses on the surface of the other side of the sheet. This phenomenon causes significant problems in achieving the expected flatness after processing flat parts. For thicker plates, this phenomenon occurs less, as the residual stress values are too low to deform a component with a larger cross-section.^[7] Diaz et al.^[18] have shown that the high speed milling process also leaves residual stresses on the machined surface. The value of these residual stresses depends on the depth of cut of the process, but also on the direction of the cold rolling process in



relation to the direction of feed speed milling process. Sedlak et al.^[19] have confirmed this phenomenon for face milling. They also showed that the residual stress values and the flatness of the machined surface are influenced not only by the cutting parameters but also by the diameter of the tool used. Zhang et al.^[20] proposed a model to optimize machining in order to minimize the impact of residual stresses created by the cutting process. Rafey Khan et al.^[21] presented ways to remove residual stresses created by the cutting process. This method involves re-heating the workpiece, which increases manufacturing costs and reduces the mechanical properties of the material. Pimenov et al.^[22] proposed method of modeling flatness deviations for face milling process. This model shows that the stiffness of the technological system has a large influence on the values of flatness deviations. On the other hand, the stiffness of the technological system is significantly affected by tool wear,^[23] which causes an increase in cutting forces.^[24] However, this model did not take into account materials produced using the cold rolling process. The extensive analysis of the effect the parameters of the aluminium alloy milling process on the cutting forces was carried out in the works.^[25-26] The works^[27-28] have shown that the strategy of face milling process is important for stability of cutting forces. Dobrzynski et al.^[29] have shown that in order to obtain the expected flatness deviations after face milling, the strategy took into account direction of feed movement in relation to the rolling direction is important.

To sum up, many studies have confirmed the occurrence of residual stresses resulting from the cold rolling process of aluminium alloy sheets. It has also been shown that the rolling direction effects the residual stress distribution. Many researchers have focused on modeling and analyzing residual stresses arising from the milling process. However, no studies to date have analyzed the effect of face milling strategies



for flat components manufactured of cold-rolled aluminium alloys sheets on the final flatness of the machined component.

The aim of these studies was to investigate, which face milling strategy would allow obtaining lower values of flatness deviation, assuming that the fixturing method and machining parameters were not changed. An optimally selected strategy of face milling of flat components allows to achieve the appropriate product quality (flatness of the surface to be machined) and to reduce manufacturing costs by reducing processing time and material waste.

Materials and methods

Materials

Cold rolling sheet plates of EN AW6082-T6 alloy were used in investigation. Samples for experimental testing were prepared with three height dimensions, H : 6, 8 and 12 mm. The sheets with nominal dimensions (1000 mm \times 2000 mm) were cut on rectangular samples with dimensions $W = 60$ mm \times $L = 200$ mm for each thickness. The cutting process was carried out on the water jet cutting machine MAXIEM 1530. This cutting method of the metal material ensures good dimensional quality and does not introduce structural changes in the material caused by temperature. The structural changes could occur during laser or plasma cutting. Circular saw cutting would require additional processing to ensure the required parallelism of the sides of the samples and surface accuracy, which are necessary for proper clamping in a vice. Samples of any thickness were prepared in two versions. The first one with the direction of cold rolling along the longer side (L_R), the second one with the direction of rolling perpendicular to the longer side (T_R) (Fig. 1).

Machine tool, tools and face milling strategies

The face milling process of samples was carried out on the milling centre AX320 Pinnacle. The movements of the tool were performed by the machine tool in accordance with the CNC program on the Heidenhain TNC 640 control system. Samples were mounted during milling process with using the standard vice with jaws length 100 mm. The depth of attachment in the jaws of vice of each sample was 3 mm. In accordance with the practice of the engineer with an elementary knowledge, the samples were supported from the bottom with steel plates during the entire milling process. These steel plates supplemented the mounting set of tested samples on the machine table (Figure 2). The face milling head equipped with 5 cutting tool inserts type APMT 160408-NA20 grade of cemented carbide K20, which is recommended to machining of aluminium alloys, was used to experimental tests. The basic dimensions of the cutting tool and cutting blade are shown in Table 1. The dimension of cutter diameter (Table 1) allowed full width processing of tested plates in one working path of the tool. The cut width was $a_e = 60$ mm. The kinematic parameters of the face milling process used during the experimental tests are shown in Table 1. These parameters have been selected based on the recommendations of the manufacturer of the cutting tool and on industrial experience in the process of face milling of front panels for server cupboard equipment, which are made of thin aluminium alloy plates in the 6xxx grade group.^[7] These kinematical parameters of milling process also take into account the small clamping surfaces of the vice's jaws to the clamped object. The clamping surfaces (3 mm × 200mm) in the jaws of the vice have been selected so that the same clamping conditions are maintained for all tested samples. An external tool cooling system integrated with milling centre AX320 was used during machining tests. In tool cooling system was used the Blasocut 2000 Universal machining fluid.



The face milling experimental tests consisted of removing a layer of material with a total thickness of $T_{\text{tot}} = 1$ mm from the aluminium alloy plates. This value was selected based on industrial practices in the process of manufacturing front panels for server rack accessories. In this process, the main surface of panel (front side) is required to be machined. For economic reasons, manufacturers strive to produce these panels with the least possible material loss. Therefore, the blank of workpiece is usually only 1 mm thicker than the target product. In addition, studies presented by Hattori et al.^[17] show that residual stresses in cold-rolled aluminium alloy products most often occur up to a depth of about 1 mm from the rolled surface. Removing process was carried out with the use of three strategies of machining. The first strategy #1 was expected to remove total thickness of material that provided to remove, only from one side of the plate – main side ($T_{\text{tot}} = T_{\text{ms}}$). The milling process in strategy #1 was realized in two steps with use two different value of cut depth (a_{p1_1} and a_{p1_2}) (Fig. 3). The strategy #2 included machining from both side of plates. In this case the layers thicknesses were symmetrically ($T_{\text{ms}} = T_{\text{bs}}$) and on each side the layer thickness was removed by two work movement with cut depth a_{p2} . Firstly, the layer of back side of plate (T_{bs}) was machined. The last strategy (#3) consisted of machining both sides, but firstly the thin layer was removed from the back side by one working movement ($T_{\text{bs}} = a_{p3_1}$). The main side was machined in work movements applied with two different cut depths: a_{p3_2} and a_{p3_3} . The all strategies were shown in Figure 3 and values of cut depths for all strategies were posted in Table 2.

Measurement methodology of flatness deviations

The measurements of flatness deviations were made on the Coordinated Measuring Machine Altera 7.5.5 of Nikon Metrology NV under control of CMM Manager v. 3.6 software. The measuring system consisted of: PH10M PLUS motorized indexing heads

and SP25M/SM25-2 scanning probe system, with 1.6 μm maximum permissible probing error and $1.8+L/400$ μm maximum permissible error for length measurement, according to ISO 10360-2:2009 ^[30] and standard temperature range $18 \div 22$ °C.

The measurement of flatness deviations for the parts under investigation includes evenly distributed 120 measuring points on the surface. The flatness deviations of samples were measured before and after the face milling process. In this case there was possibility of comparing obtained results from two series measurements and checking the face milling strategy effect on flatness deviations.

Results and discussion

Flatness deviations of the specimens with the longitudinal direction of rolling (L_R) before the milling process were in the range of 0.04 mm to 0.11 mm (Table 3). The deviations had a small spreads of values for each thickness of samples (Fig. 4) (Table 3). The shape of the surface deformations had no clear directionality (Fig. 5b). Samples with transverse direction of rolling (T_R) had higher values of flatness deviations (Table 3). In this case, this is due to the introduced anisotropy of the material as a result of cold rolling. Compressive stresses perpendicular to the rolling direction occur over a longer section of the specimen and have a significant advantage over tensile stresses directed along the rolling direction. This is particularly noticeable for a 6 mm thick specimen TR6S1 (Fig. 5a). The values of deviation for plates with thickness 6 mm was 6 times higher, and for other thicknesses around 3 times (Fig. 4) (Table 3). In case of samples with thicknesses 8 mm and 12 mm was also observed larger spreads than in the sample with longitudinal rolling (L_R) (Fig. 4). Additionally, the shape of the surface deformations for plates with thickness 6 mm was bent with a recess in the middle of the sample (U-shape). For the thicker samples the shape of deformations was wavy with two recesses along the sample length (Fig. 5a). In both cases, in the direction



of longitudinal and transverse rolling, the shape of the deformation probably depended mainly on the thickness of sample and stress on the outer surface resulting from the cold rolling process.

The values of flatness deviations after milling process for samples with longitudinal rolling direction were measured in range between 0.022 mm to 0.102 mm (Table 4). While for samples with transverse rolling direction were in range 0.025 mm to 0.289 mm (Fig. 6). The strategy #1 consisted of material removal only from one side. In effect these cases gave more deformed of plate (degradation of flatness values) because the residual surface stresses were removed only from machined side of plate. The residual stresses from non-machined side did not have balancing stresses and then those were affected more by deformation of samples. On the other side, the strategy #1 consisted of material removal only from one side. In effect this cases gave more deformed of plate (degradation of flatness values) because the residual surface stresses were removal only from machined side of plate. The residual stresses from non machined side did not have balancing stresses and them were affected more deformation of samples. This phenomenon was especially observed for samples with longitudinal rolling direction. In those cases, non symmetrical dimensions of samples, $L \gg W$ (Fig. 1) could affect value of deformation because of direction of grain effect on distribution of surface stresses. Of course, proportional sample dimensions could change only shape of deformation not the value. The use of strategy #3 in the face milling process resulted in a noticeably better improvement in flatness. Improvement was achieved for each thicknesses of samples and also for both rolling directions. This phenomenon was caused by symmetrical (both side of plate) removal of material with residual surface stresses.^[13-17] The thickness of the samples tested also had an impact on the results obtained and for thicker samples (8 mm and 12 mm) the flatness values were similar for both rolling directions, in range



0.022 mm to 0.102 mm. This may indicate that the residual stress values remaining in the material after processing are too small to deform a component with such a large thickness. The flatness deviations almost only for plates with 6 mm thickness and transverse rolling direction were notably higher (Fig. 6). Those height values were in range 0.264 mm to 0.289 mm and presented very low spread between strategies.

The transverse rolling direction in relation to the longer side of the specimen and the significant difference in the dimensions of the length and width of the specimen directly affects the spread of flatness values both after rolling and after milling. This may be due to a higher proportion of residual compressive stress. This anisotropy of the material as seen has a dominant influence, independent of the thickness of the specimen because the largest spread between flatness values were obtained for plates with thickness 8 mm both after rolling and after milling. In this case the spread of flatness deviations was about 0.170 mm (Fig. 6) after milling process and about 0.360 mm (Fig. 4) after transverse rolling. The deformation shape of the tested samples was preserved, which can be seen in Fig. 5 and Fig. 7. This phenomenon was obtained for samples with both rolling direction.

Generally, the face milling process for almost each analyzed strategy caused reduced values of flatness deviations on average by 0.05 mm (Fig. 8 and 9). The biggest reduction of flatness was obtained for milling strategy #3 in case of samples with transversal rolling direction (Fig. 9). Those samples had the highest values of flatness deviations before milling process. Whereas, after the face milling process with strategy #3, deviations were improved by up to 0.25 mm for sample with 8 mm thickness.

However, for samples with longitudinal rolling direction, where before milling process the values of flatness deviations were very low, obtained a small improvement in flatness (about 0.04 mm) for #2 and #3 strategies (Fig. 8). Even in #1 strategy case the



flatness was worsened (Fig. 8) for each plate thicknesses. On the basis of the obtained results, it can be seen that an important aspect is the removal of residual surface stresses symmetrically on both sides of the plates (strategy # 3). This approach is especially important for components made of thin metal sheets up to about 6 mm thick. In the case of thicker plates, asymmetric residual stress relief on both sides of the plate also works well (strategy # 2). The remaining residual stresses are not high enough to distort the component.

Conclusions

Based on the carried out experimental tests and analyses of obtained results, it can be concluded that:

- the direction of rolling process for AW 6082-T6 alloy can have an effect on values of flatness deviations after face milling process;
- the thickness dimension of AW 6082-T6 alloy samples have effect on values of flatness deviations after face milling process;
- in order to obtain the expected values of flatness deviations after the face milling process of AW 6082-T6 alloy plates with thickness dimensions up to 12 mm, a strategy of machining is important;
- the strategy of face milling process consisting of symmetrical removal material from both side of plate has given the best results of flatness for tested plates AW 6082-T6 alloy.

Acknowledgements

The authors would like to acknowledge Eng. Roman Jakubek and MSc. Eng. Jan Westa from the company Mechanika - Radmor Sp. z o.o. in Gdynia, Poland, for supplying materials for this work and substantive consultations.

References

- [1] Hu, H., Yu, A., Li, N., Allison, J.E. Potential Magnesium Alloys for High Temperature Die Cast Automotive Applications: A Review. *Mater. Manuf. Processes* **2003**, *18*(5), 687-717. DOI: 10.1081/AMP-120024970
- [2] Miller, W.S., Zhuang, L., Bottema, J., Wittebrood, A.J., De Smet, P., Haszler, A., Vieregge, A. Recent Development in Aluminium Alloys for the Automotive Industry. *Mat. Sci. Eng. A-Struct.* **2000**, *280*(1), 37–49. DOI: 10.1016/S0921-5093(99)00653-X
- [3] Hirsch, J. Recent Development in Aluminium for Automotive Applications. *T. Nonferr. Metal Soc.* **2014**, *24*(7), 1995-2002. DOI: 10.1016/S1003-6326(14)63305-7
- [4] Heinz, A., Haszler, A., Keidel, C., Moldenhauer, S., Benedictus, R., Miller, W.S. Recent Development in Aluminium Alloys for Aerospace Applications. *Mat. Sci. Eng. A-Struct.* **2000**, *280*(1), 102–107. DOI: 10.1016/S0921-5093(99)00674-7
- [5] Starke Jr., E.A., Staley, J.T. Application of Modern Aluminum Alloys to Aircraft. *Prog. Aerosp. Sci.* **1996**, *32*(2-3), 131-172. DOI: 10.1016/0376-0421(95)00004-6
- [6] Goni, J., Egizabal, P., Coletto, J., Mitxelena, I., Leunda, I., Guridi, R.J. High performance automotive and railway components made from novel competitive aluminium composites. *Mater. Sci. Tech.* **2003**, *19*(7), 931-934. DOI: 10.1179/026708303225004413
- [7] Personal Source **2019**. Consultation with MSc. Eng. Jan Westa, Head of the Technology Department of Mechanika-Radmor Co., Gdynia, Poland.
- [8] ISO 6361-4:2014. Wrought Aluminium and Aluminium Alloys — Sheets, Strips and Plates — Part 4: Sheets and Plates: Tolerances On Shape and Dimensions. *The International Organization for Standardization*, Geneva, Switzerland.



- [9] Umamaheshwer Rao, A.C., Vasu, V., Govindaraju, M., Sai Srinadh, K.V. Influence of Cold Rolling and Annealing on the Tensile Properties of Aluminium 7075 Alloy. *Procedia Mater. Sci.* **2014**, 5, 86-95.
- [10] Wang, B., Chen, X., Pan, F., Mao, J., Fang, Y. Effects of Cold Rolling and Heat Treatment on Microstructure and Mechanical Properties of AA 5052 Aluminum Alloy. *Trans. Nonferrous Met. Soc. China* **2015**, 25, 2481-2489.
- [11] Aleksandrović, S., Stefanović, M., Adamović, D., Lazić, V. Variation of Normal Anisotropy Ratio "r" During Plastic Forming. *Stroj. Vestn. – J. Mech. E.* **2009**, 55(6). 392-399.
- [12] Najib, L.M., Alisibramulisi, A., Amin, N.M., Bakar, I.A.A., Hasim, S. The Effect of Rolling Direction to the Tensile Properties of AA5083 Specimen. In: *InCIEC 2014: Innovative Construction Materials and Structures*; Hassan, R., Yusoff, M., Alisibramulisi, A., Mohd Amin, N., Ismail, Z. Ed.; Springer: Singapore, **2015**. DOI: 10.1007/978-981-287-290-6_67
- [13] Robinson, J.S., Pirling, T., Truman, C.E., Panzner, T. Residual stress relief in the aluminium alloy 7075. *Mater. Manuf. Processes* **2017**. 33(15), 1765-1775. DOI: 10.1080/02670836.2017.1318243
- [14] Pan, R., Zheng, J., Zhang, Z., Lin, J. Cold rolling influence on residual stresses evolution in heat-treated AA7xxx T-section panels. *Mater. Manuf. Processes* **2019**, 34(4), 431-446. DOI: 10.1080/10426914.2018.1512121
- [15] Ye, N.-Y., Cheng, M., Zhang, S.-H. Effect of Cold Rolling Parameters on The Longitudinal Residual Stress Distribution of GH4169 Alloy Sheet. *Acta Metall. Sin. (Engl. Lett.)* **2015**, 28(12), 1510-1517. DOI: 10.1007/s40195-015-0351-4



- [16] Ding, Z. H., Cui, F. K., Liu, Y. B., Li, Y., Xie, K. G. A Model of Surface Residual Stress Distribution of Cold Rolling Spline. *Hindawi Math. Probl. Eng.* **2017**, 21. DOI: 10.1155/2017/2425645
- [17] Hattori, N., Matsumoto, R., Utsunomiya, H. Residual Stress Distribution Through Thickness in Cold-Rolled Aluminum Sheet. *Key Eng. Mater.* **2014**, 622-623, 1000-1007. DOI:10.4028/www.scientific.net/KEM.622-623.1000
- [18] Díaz, F., Mammana, C., Guidobono, A. Evaluation of Residual Stresses Induced by High Speed Milling Using an Indentation Method. *Mod. Mech. Eng.* **2012**, 2, 143-150. DOI: 10.4236/mme.2012.24019
- [19] Sedlak, J., Osicka, P., Chladil, J., Jaros, A., Polzer, A. Residual Stress When Face Milling Aluminium Alloys. *MM Sci. J.* **2018**, 11, 2530-2535. DOI: 10.17973/MMSJ.2018_11_201821
- [20] Zhang, Q., Mahfouf, M., Yates, R.J., Pinna, C., Panoutsos, G., Boumaiza, S., Greene, R.J., de Leon, L. Modeling and Optimal Design of Machining-Induced Residual Stresses in Aluminium Alloys Using a Fast Hierarchical Multiobjective Optimization Algorithm. *Mater. Manuf. Processes* **2011**. 26(3), 508-520. DOI: 10.1080/10426914.2010.537421
- [21] Rafey Khan, A., Nisar, S., Shah, A., Khan, M.A., Khan, S.Z., Sheikh, M.A. Reducing Machining Distortion in AA 6061 Alloy Through Re-heating Technique. *Mater. Sci. Tech.* **2017**, 33(6), 731-737. DOI: 10.1080/02670836.2016.1243335
- [22] Pimenov, D.Y., Guzeev, V.I., Krolczyk, G., Mia, M., Wojciechowski, S. Modeling Flatness Deviation in Face Milling Considering Angular Movement of the Machine Tool System Components and Tool Flank Wear. *Precis. Eng.* **2018**, 54, 327–337. DOI: 10.1016/j.precisioneng.2018.07.001



- [23] Pimenov, D. Y., Guzeev, V. I., Mikolajczyk, T., Patra, K. A Study of the Influence of Processing Parameters and Tool Wear on Elastic Displacements of the Technological System Under Face Milling. *Int. J. Adv. Manuf. Technol.* **2017**, *92*, 4473-4486. DOI: 10.1007/s00170-017-0516-6
- [24] Guzeev, V. I., Pimenov, D. Yu. Cutting Force in Face Milling With Tool Wear. *Russian Engineering Research* **2011**, *31*(10), 989–993.
- [25] Jebaraj, M., Pradeep Kumar, M., Yuvaraj, N., & Mujibar Rahman, G. Experimental Study of the Influence of the Process Parameters in the Milling of Al6082-T6 Alloy. *Mater. Manuf. Processes* **2019**, *34*(12), 1411-1427. DOI: 10.1080/10426914.2019.1594271
- [26] Jebaraj, M., Pradeep Kumar, M. Effect of Cryogenic CO₂ and LN₂ Coolants in Milling of Aluminum Alloy. *Mater. Manuf. Processes* **2019**, *34*(5), 511-520. DOI: 10.1080/10426914.2018.1532591
- [27] Bagci, E., Yüncüoğlu, E. U. The Effects of Milling Strategies on Forces, Material Removal Rate, Tool Deflection, and Surface Errors for the Rough Machining of Complex Surfaces. *Stroj. Vestn. – J. Mech. E.* **2017**, *63*(11), 643-656. DOI:10.5545/sv-jme.2017.4450
- [28] Jarosz, K., Löschner, P., Nieslony, P., Krolczyk, G. Optimization of CNC Face Milling Process of Al-6061-T6 Aluminum Alloy. *J. Mach. Eng.* **2017**, *17*(1), 69-77.
- [29] Dobrzynski, M., Chuchala, D., Orlowski, K. A. The Effect of Alternative Cutter Paths on Flatness Deviations in the Face Milling of Aluminum Plate Parts. *J. Mach. Eng.* **2018**, *18*(1), 80-87.
- [30] ISO 10360-2:2009. Geometrical Product Specifications (GPS) – Acceptance and Reverification Tests for Coordinate Measuring Machines (CMM) – Part 2: CMMs Used for



Measuring Linear Dimensions. *The International Organization for Standardization*,
Geneva, Switzerland.

Figure captions:

Figure 1. Rolling directions for tested aluminium alloys samples. L_R – longitudinal rolling direction; T_R – transverse rolling direction; L – length of sample; W – width of sample

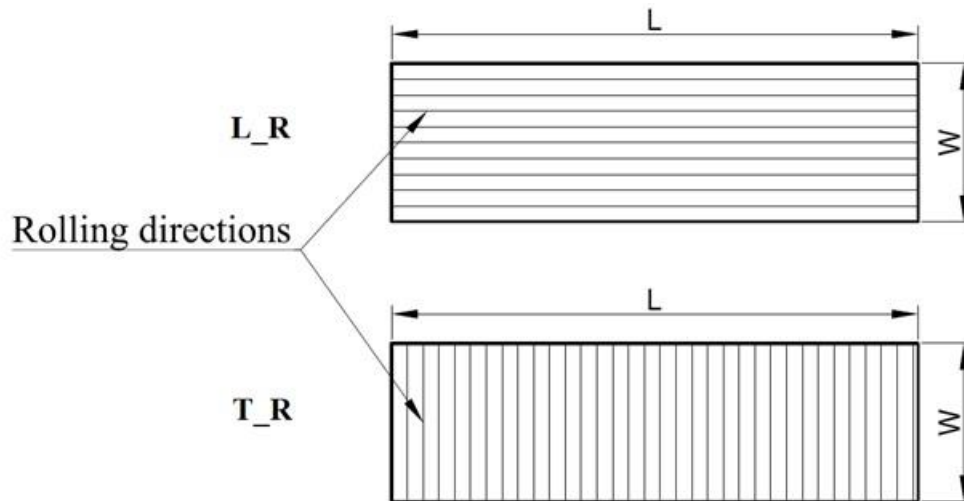
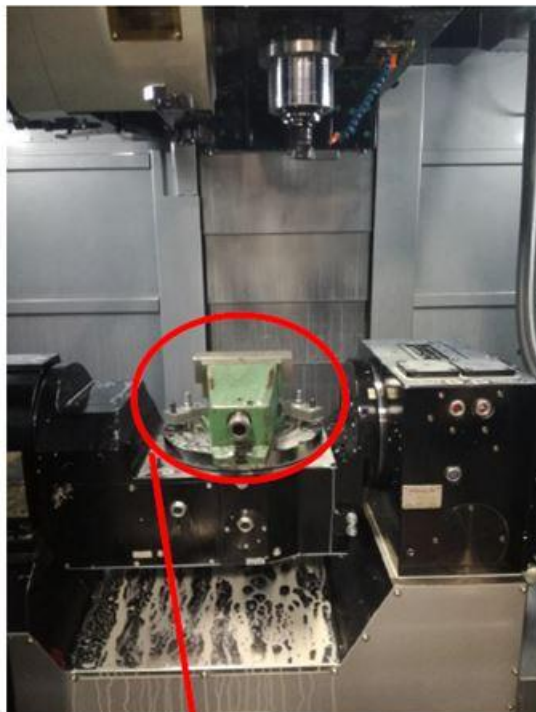


Figure 2. Machine tool with equipment for machining tests: a) view on work zone of machine tool, b) sample clamped in a vice

a)



b)

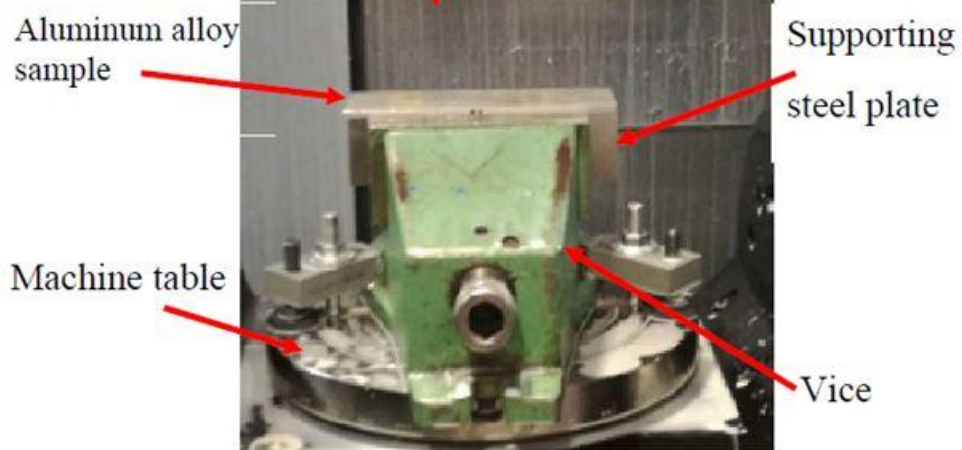


Figure 3. Three experimental research strategies for face milling of aluminium alloy plates

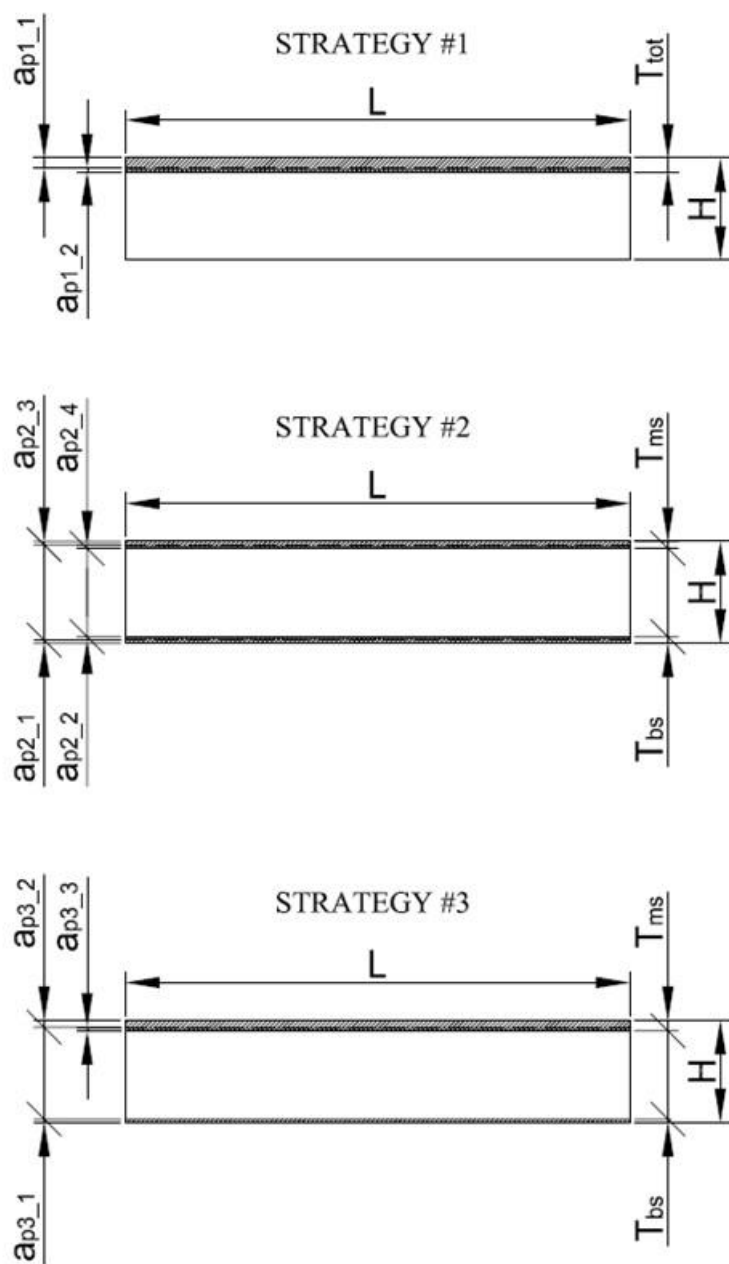


Figure 4. Flatness of the surface after rolling process (before face milling process)

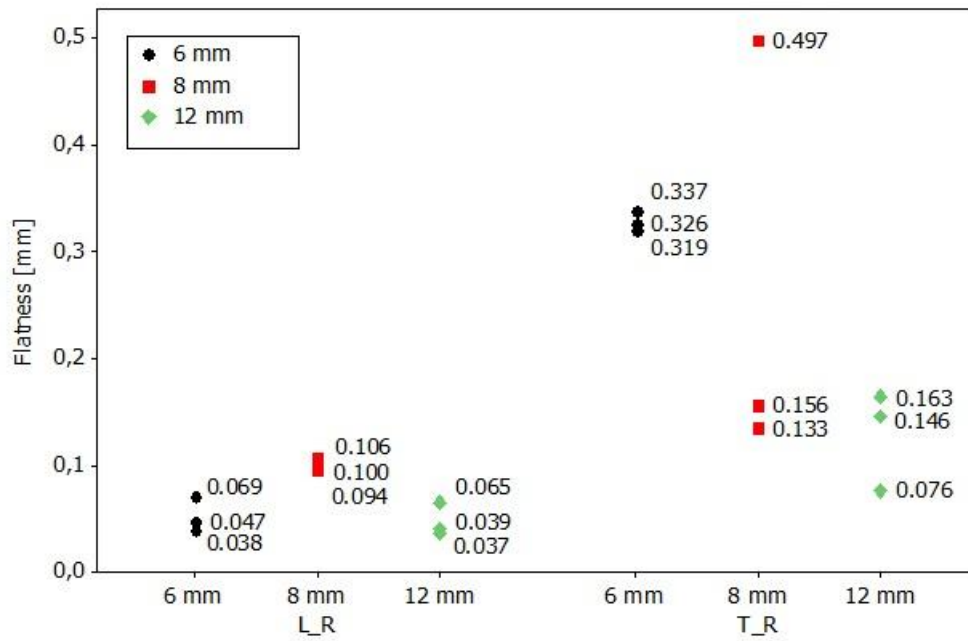


Figure 5. The shape of the deformation after rolling process (before face milling) for selected samples. TR6S1 – sample with transverse rolling direction, 6 mm thickness, prepared for milling strategy #1. LR – longitudinal rolling direction

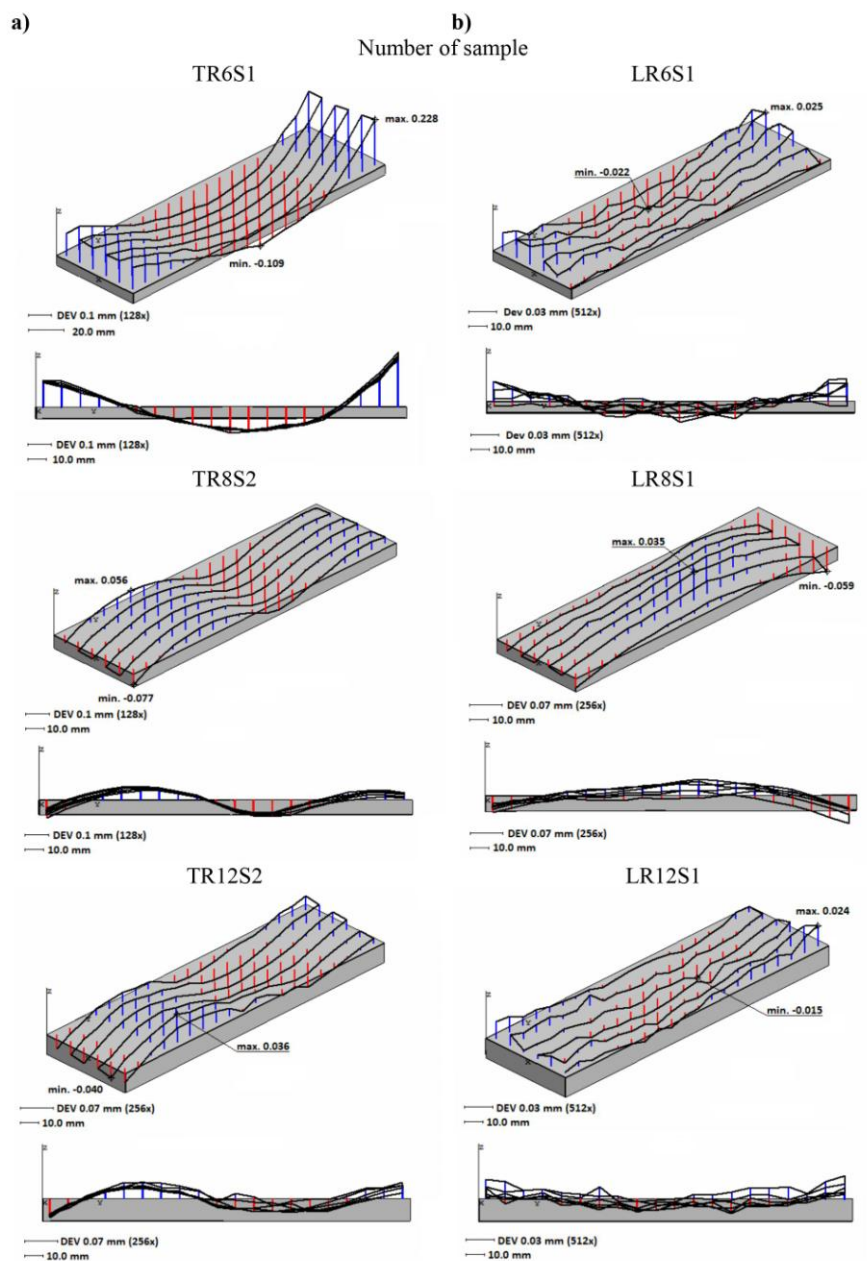


Figure 6. Flatness of the surface after milling process

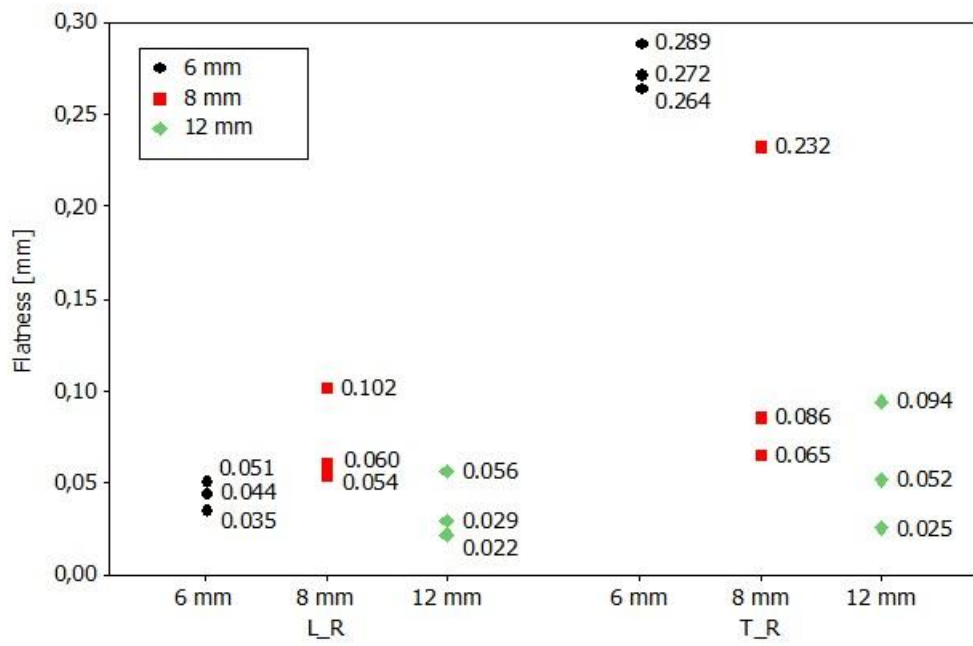


Figure 7. The shape of the deformation after face milling process for selected samples. TR6S1 – sample with transverse rolling direction, 6 mm thickness, prepared for milling strategy #1. LR – longitudinal rolling direction.

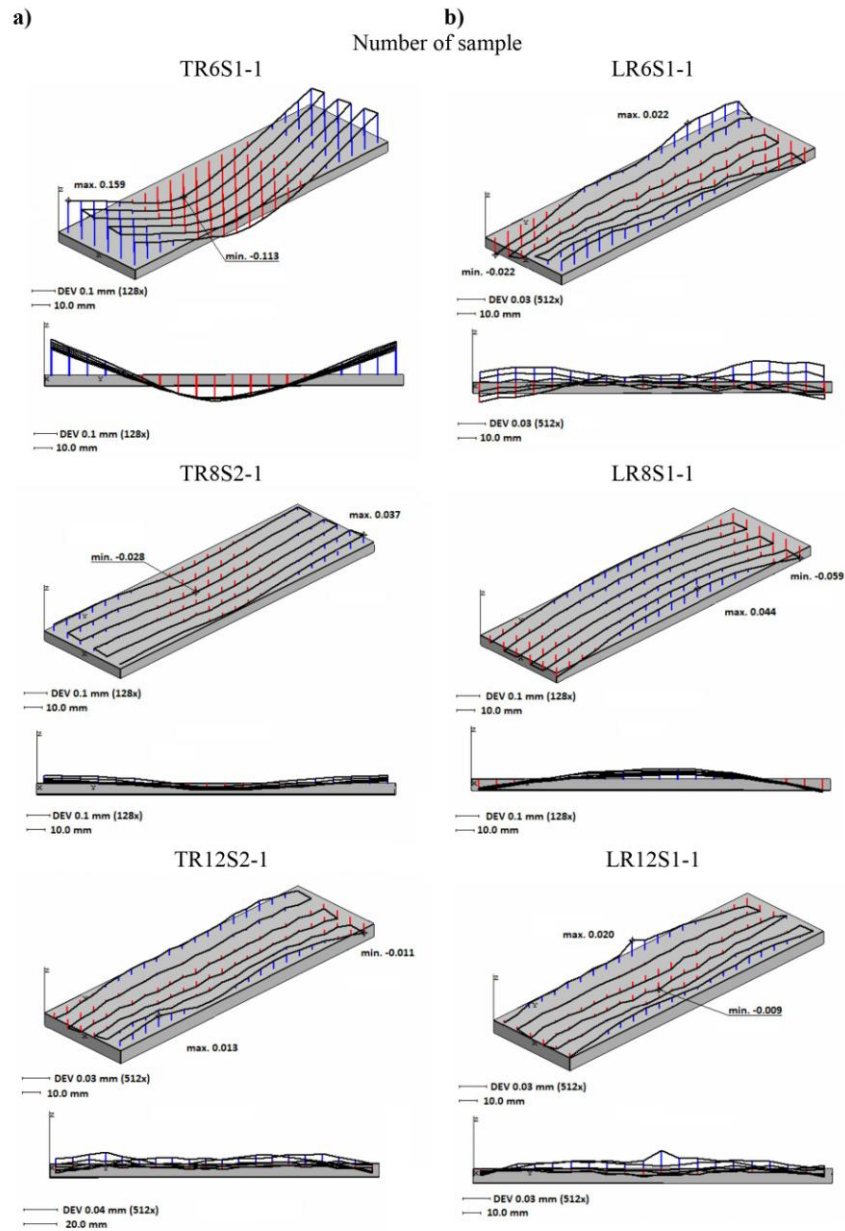


Figure 8. Differences between the flatness of samples before milling and after face milling using three strategies(S#1, S#2, S#3), for samples of three different thicknesses with longitudinal rolling direction (L_R)

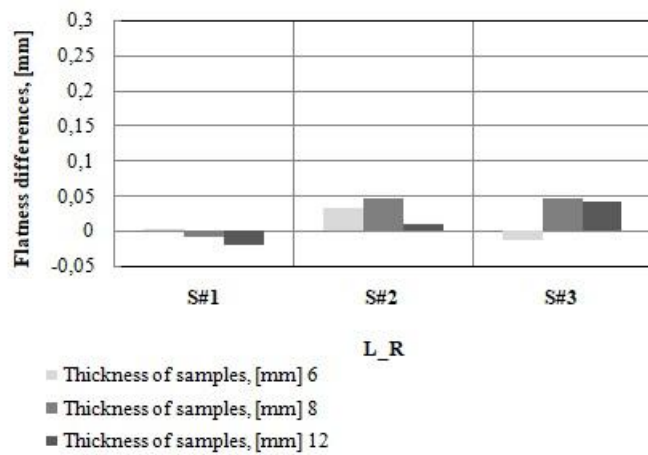


Figure 9. Differences between the flatness of samples before milling and after face milling using three strategies(S#1, S#2, S#3), for samples of three different thicknesses with transverse rolling direction (T_R)

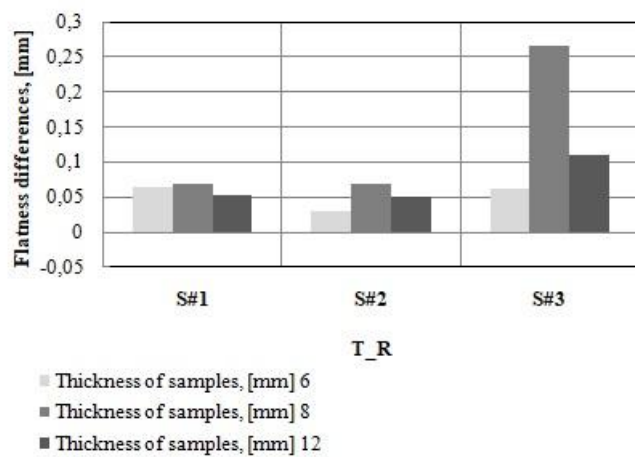


Table 1. The basic parameters of the cutting tool and milling process.

Name of dimension	Value	Unit
Cutting tool and cutting blade		
Diameter of milling head, D	63	mm
Number of blades (inserts), z	5	-
Corner radius, r_o	0.8	mm
Tool rake angle, γ_f	10	°
Tool minor rake angle, γ_f'	10	°
Tool clearance angle, α_f	11	°
Tool minor clearance angle, α_f'	15	°
Tool cutting edge angle, κ_r	90	°
Tool minor cutting edge angle, κ_r'	90	°
Milling process		
Rotation speed, n	1400	min^{-1}
Cutting speed, v_c	264	$\text{m} \cdot \text{min}^{-1}$
Feed speed, v_f	600	$\text{mm} \cdot \text{min}^{-1}$
Feed per tooth, f_z	0.086	mm



Table 2. Cut depths for investigated strategies.

Name of strategy	Machining side of plates	Value of thickness layer [mm]	Symbol of cut depth	Value of cut depth [mm]
Strategy #1	main side, T_{ms}	1.00	a_{p1_1}	0.75
			a_{p1_2}	0.25
Strategy #2	back side, T_{bs}	0.50	a_{p2_1}	0.25
			a_{p2_2}	0.25
	main side, T_{ms}	0.50	a_{p2_3}	0.25
			a_{p2_4}	0.25
Strategy #3	back side, T_{bs}	0.25	a_{p3_1}	0.25
	main side, T_{ms}	0.75	a_{p3_2}	0.50
			a_{p3_3}	0.25

Table 3. Measuring results and main statistics of the surface flatness after rolling process

Rolling strategy	Thickness of the sample [mm]	Milling strategy	Flatness [mm]	Max deviation [mm]	Min deviation [mm]	RMS
T_R	6	S#1	0.337	0.228	-0.109	0.086
T_R	6	S#2	0.319	0.217	-0.102	0.085
T_R	6	S#3	0.326	0.219	-0.107	0.084
L_R	6	S#1	0.047	0.025	-0.022	0.010
L_R	6	S#2	0.069	0.026	-0.044	0.014
L_R	6	S#3	0.038	0.021	-0.017	0.007
T_R	8	S#1	0.156	0.059	-0.096	0.039
T_R	8	S#2	0.133	0.056	-0.077	0.037
T_R	8	S#3	0.497	0.187	-0.310	0.156
L_R	8	S#1	0.094	0.035	-0.059	0.018
L_R	8	S#2	0.100	0.035	-0.065	0.024
L_R	8	S#3	0.106	0.043	-0.063	0.026
T_R	12	S#1	0.146	0.055	-0.091	0.033
T_R	12	S#2	0.076	0.036	-0.040	0.020
T_R	12	S#3	0.163	0.055	-0.108	0.038
L_R	12	S#1	0.037	0.023	-0.014	0.008
L_R	12	S#2	0.039	0.024	-0.015	0.008
L_R	12	S#3	0.065	0.047	-0.018	0.009

Table 4. Measuring results and main statistics of the surface flatness after face milling process

Rolling strategy	Thickness of the sample [mm]	Milling strategy	Flatness [mm]	Max deviation [mm]	Min deviation [mm]	RMS
T_R	6 mm	S#1	0.272	0.159	-0.113	0.078
T_R	6 mm	S#2	0.289	0.157	-0.131	0.082
T_R	6 mm	S#3	0.264	0.151	-0.114	0.081
L_R	6 mm	S#1	0.044	0.022	-0.022	0.009
L_R	6 mm	S#2	0.035	0.022	-0.013	0.007
L_R	6 mm	S#3	0.051	0.025	-0.026	0.015
T_R	8 mm	S#1	0.086	0.046	-0.040	0.023
T_R	8 mm	S#2	0.065	0.037	-0.028	0.017
T_R	8 mm	S#3	0.232	0.098	-0.134	0.066
L_R	8 mm	S#1	0.102	0.044	-0.059	0.026
L_R	8 mm	S#2	0.054	0.028	-0.026	0.012
L_R	8 mm	S#3	0.060	0.028	-0.032	0.012
T_R	12 mm	S#1	0.094	0.039	-0.055	0.022
T_R	12 mm	S#2	0.025	0.013	-0.011	0.005
T_R	12 mm	S#3	0.052	0.023	-0.029	0.013
L_R	12 mm	S#1	0.056	0.025	-0.031	0.014
L_R	12 mm	S#2	0.029	0.020	-0.009	0.005
L_R	12 mm	S#3	0.022	0.011	-0.011	0.005

